

Article

# Shape Design of the Duct for Tidal Converters Using Both Numerical and Experimental Approaches (pre-2015)

Chul H. Jo, Do Y. Kim, Su J. Hwang and Chan H. Goo \*

Department of Naval Architecture and Ocean Engineering, Inha University, Incheon 22212, Korea; chjo@inha.ac.kr (C.H.J.); doyoubkim815@inha.edu (D.Y.K.); sjhwang@inha.edu (S.J.H.)

\* Correspondence: chanhoegoo@inha.edu; Tel.: +82-32-860-8849; Fax: +82-32-864-5850

Academic Editor: Jang-Ho Lee

Received: 23 December 2015; Accepted: 29 February 2016; Published: 11 March 2016

**Abstract:** Recently, focus has been placed on ocean energy resources because environmental concerns regarding the exploitation of hydrocarbons are increasing. Among the various ocean energy sources, tidal current power (TCP) is recognized as the most promising energy source in terms of predictability and reliability. The enormous energy potential in TCP fields has been exploited by installing TCP systems. The flow velocity is the most important factor for power estimation of a tidal current power system. The kinetic energy of the flow is proportional to the cube of the flow's velocity, and velocity is a critical variable in the performance of the system. Since the duct can accelerate the flow velocity, its use could expand the applicable areas of tidal devices to relatively low velocity sites. The inclined angle of the duct and the shapes of inlet and outlet affect the acceleration rates of the flow inside the duct. In addition, the volume of the duct can affect the flow velocity amplification performance. To investigate the effects of parameters that increase the flow velocity, a series of simulations are performed using the commercial computational fluid dynamics (CFD) code ANSYS-CFX. Experimental investigations were conducted using a circulation water channel (CWC).

**Keywords:** tidal current power (TCP); duct; circulation water channel (CWC); horizontal axis tidal turbine; ocean energy; experiment

## 1. Introduction

Tidal current power (TCP) from ocean energy has huge potential throughout the world. It is a very reliable and predictable resource. Therefore many researches have been performed regarding applications of tidal current power systems for example Bahaj *et al.* [1], and Batten *et al.* [2].

Flow velocity is the most critical factor for power generation from tidal currents since the kinetic energy of the flow stream is proportional to the cube of the flow velocity. Among several types of current turbine systems, the application of duct could increase the upstream velocities and the power extraction from the current. Numerous researches have been presented regarding duct applications for TCP systems [3]. Several experimental studies on a ducted horizontal axis turbine (HAT) system were conducted [4]. The effect of the diffuser angle which is the angle between cylindrical duct wall and diffuser duct wall on ducted turbine performance was described [5]. Computational fluid dynamics (CFD) analyses of the effects on inlet shapes on the inside velocity of a duct were carried out [6]. A duct system using hydrofoil sections around the turbine was introduced in 2013.

Typically, strong current speeds above 2.5 m/s are considered favorable to generate from tidal current energy [7], but lower-flow tidal turbine technologies essential for the development of the industry. The application of ducts can accelerate the flow velocity, and can potentially broaden the applicable areas of tidal devices to relatively lower velocity sites. In many researches, it has been proven that a duct could enhance the amount of power production by amplifying the flow velocity, but the duct should be designed by considering the specific environmental conditions and the whole

concept of the structure. This paper describes the preliminary design of a duct that can be applied to a tidal current power system moored to a seabed and the flow characteristics around the duct based on CFD analyses. Experimental studies were carried out to validate the CFD results.

## 2. Overall System Concept

Many sites (such as a drain channel in a conventional power plant and islands areas) have a relatively lower current velocity. A single point mooring system could be applied to a TCP system with a duct structure for easy installation and maintenance [8]. As shown in Figure 1, a single point mooring system needs buoyancy for mooring, so the duct should be designed with enough bulk to act as ballasting tank. Some generating devices and a power train could be placed in this space [9]. The duct design was initiated considering the overall concept of the generating system.

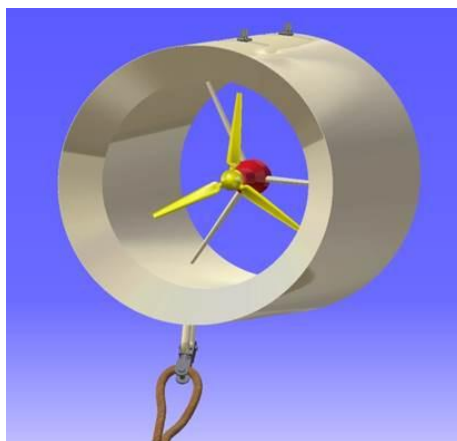


Figure 1. Schematic view of TCP with a single point mooring system.

## 3. Duct Design

The angle of duct was based on a previous study [5]. Thin plate shape shrouded ducts were analyzed by CFD. The optimal angle of nozzle and diffuser,  $18.05^\circ$  had been defined. In later research, three types of ducts were designed considering the entire concept of a single point moored TCP. A nozzle-diffuser type duct that has  $11.2^\circ$  of nozzle and diffuser angle showed the highest performance with 1.65 flow amplification factor. In [10], a CFD analysis for that nozzle-diffuser type duct including counter-rotating turbine was conducted as shown in Figure 2. However the turbine inside the duct blocked and disturbed the flow into the duct, and the turbine performance was not enhanced significantly. Therefore the study on modification for duct shape was conducted based on this previous CFD analyses. In this study, the nozzle-diffuser type duct was called to baseline duct.

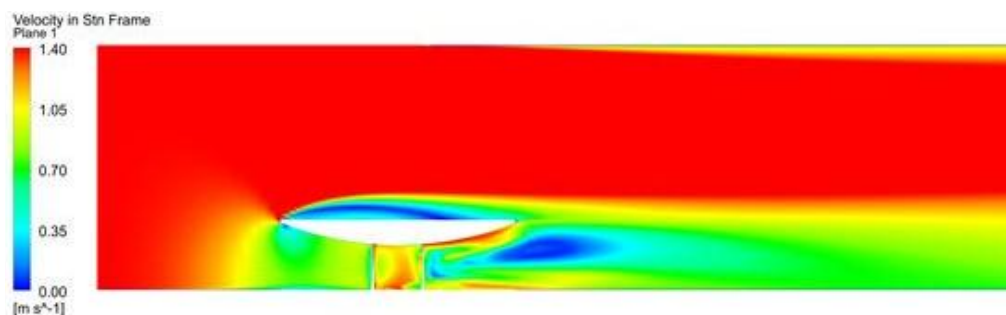


Figure 2. CFD result of the baseline duct with turbine [8].

To improve the duct performance, two methods were considered. The first method is to modify the diffuser angle. With using the shape of the baseline duct, several CFD analyses were carried out to investigate the performance of the duct with various diffuser angles. For the results, the  $5^\circ$  case was defined as the optimal diffuser angle. That case showed the maximum flow amplification factor of 1.82. Another method is to modify the shape of the outer surface to prevent separation near the inlet. Therefore three modified ducts were designed based on the baseline duct shape. The modified duct shapes are shown in Figure 3.

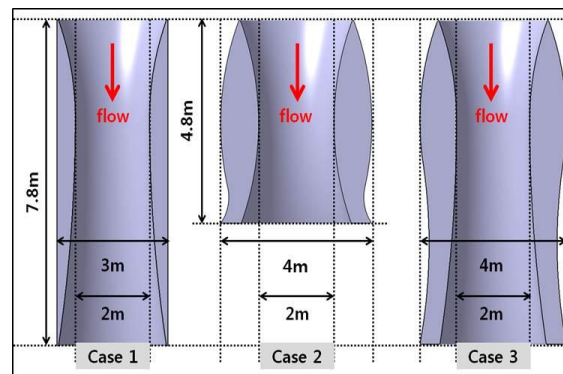


Figure 3. 3-D duct design with CATIA V5R19.

Case 1 has  $5^\circ$  of diffuser angle. Case 2 has a curved surface to prevent the separation observed in CFD analysis including a tidal turbine. Both the modified diffuser angle and curved surface, were applied to Case 3 to examine the combined effect on the duct performance. Also, Case 2 and Case 3 have cut outlet shapes to generate negative pressure behind the outlet due to suction effects.

#### 4. CFD Analysis

This research used the ANSYS CFX v13.0 commercial CFD code to simulate flow patterns around the three duct shapes. All analysis cases have the same external boundary dimensions as shown in Figure 4, with different duct shapes in the inner domain.

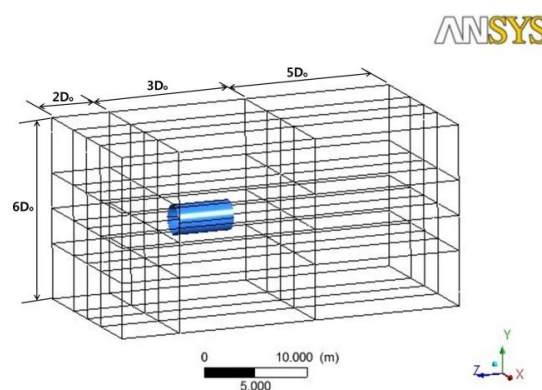


Figure 4. External boundary dimensions.

Grid generation was carefully carried out for smooth convergence and reliable results. The thickness of the near-wall grid layers was considered according to the application of the turbulence model, as was the aspect ratio of the mesh. In this simulation, a shear stress transport (SST) model, which requires a low  $y$ -plus value under 10 for reliable results, was used as the turbulence closure. A total of 2 million nodes were generated with tetrahedral and prism cells. Table 1 shows the computational grid information.

**Table 1.** Analysis conditions.

Description	Analysis Condition
Working fluid	Water (1025 kg/m <sup>3</sup> )
Inlet	Normal speed (2 m/s)
Wall	Stationary wall (no slip)
Outlet	Outlet (Relative pressure = 0 Pa)
Turbulence model	SST model

Figure 5 shows the characteristics around the duct from the CFD analyses. For all cases, flow velocities inside the duct were amplified more than in the baseline duct. Huge vortices were observed near the outlet in Case 2 and Case 3 due to the cut outlet shapes. Also the location where the maximum flow velocity was generated was found for each case. One may describe the flow pattern through the pressure distributions. The stagnation pressure near inlet decreased more than in the baseline duct. Negative pressures were observed near the outlet in Case 2 and Case 3. These negative pressures can contribute to the duct performance with suction effects.

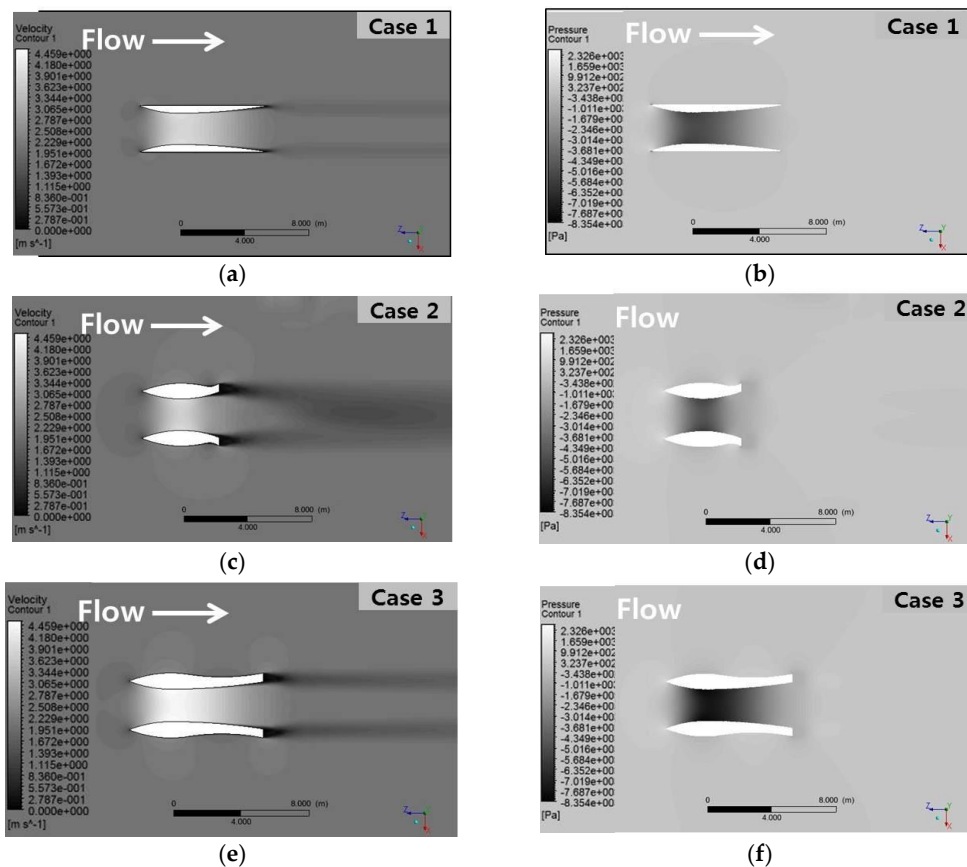


**Figure 5.** Flow characteristics around the each duct. (a) Velocity field of Case 1; (b) Pressure distribution of Case 1; (c) Velocity field of Case 2; (d) Pressure distribution of Case 2; (e) Velocity field of Case 3; (f) Pressure distribution of Case 3.

In particular, the maximum flow amplification factor was 2.14 in Case 3. Figure 6 is a comparison of the maximum flow amplification factors for each case. From the CFD analysis, a remarkable improvement was found. From the baseline duct shape, the duct performance has been enhanced significantly through the modification. These flow amplification factors are the ratio of maximum velocity inside the duct and the upstream flow velocity.

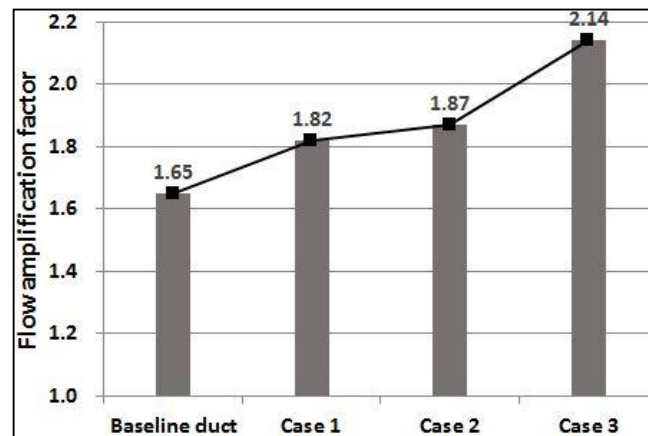


Figure 6. Comparison of maximum flow amplification factor in the duct.

## 5. Experimental Validation

To validate the results of CFD, experiments were conducted in a circulation water channel. Three type of 1/6 scale duct mock-ups were manufactured as shown in Figure 7. To measure the velocity inside the duct, an acoustic Doppler velocimeter (ADV) was used. Each duct mock-up has several accessible slits to insert the ADV's stem.

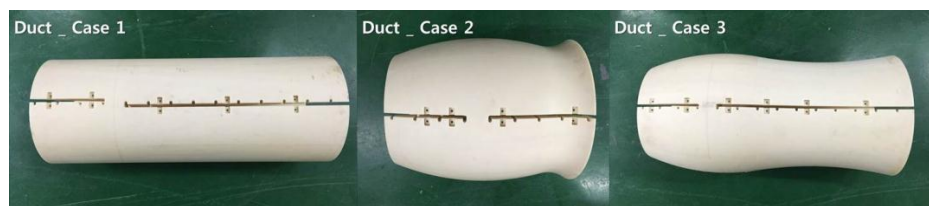


Figure 7. Three case mock-ups.

The experiments were carried out with 1.0 m/s upstream and 0.78 m water depth conditions. As shown in Figure 8, the duct mock-up was supported by a stainless steel structure.



Figure 8. Installed duct mock-up.

The inflow area in the circulation water channel is  $0.78 \text{ m}^2$ . The blockage ratio of each duct model was 0.15 (Case 1) and 0.379 (Case 2 and Case 3). Obtained experimental data was plotted in Figure 9.

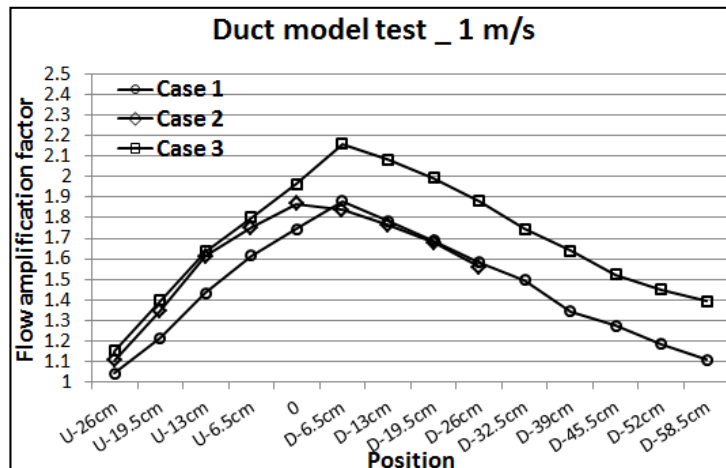


Figure 9. Flow amplification factor according to location in the duct.

0 point is where inner diameter is minimum, “U” means upstream direction and “D” means downstream direction. The maximum flow amplification factor of case 1 was 1.86. For Case 2, the value was similar (1.88). In Case 3, the maximum flow amplification factor was 2.15. Also, it was found that the location where the maximum flow velocities were generated were different for Case 1 and Case 3. Figures 10–12 show the comparison of CFD and experiment results.

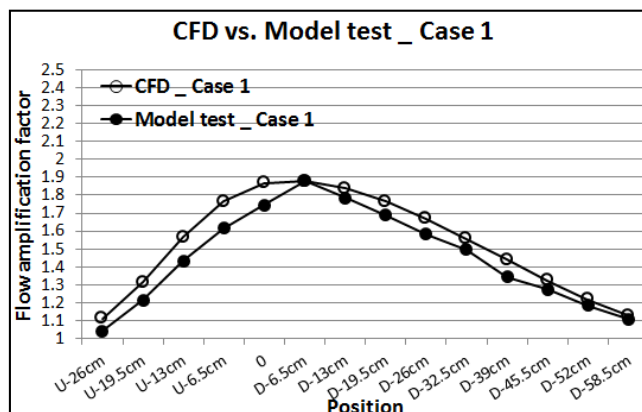


Figure 10. Comparison of CFD and experiment in Case 1.

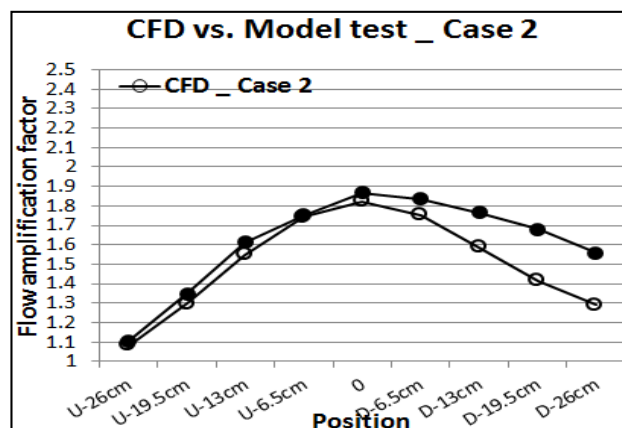


Figure 11. Comparison of CFD and experiment in Case 2.

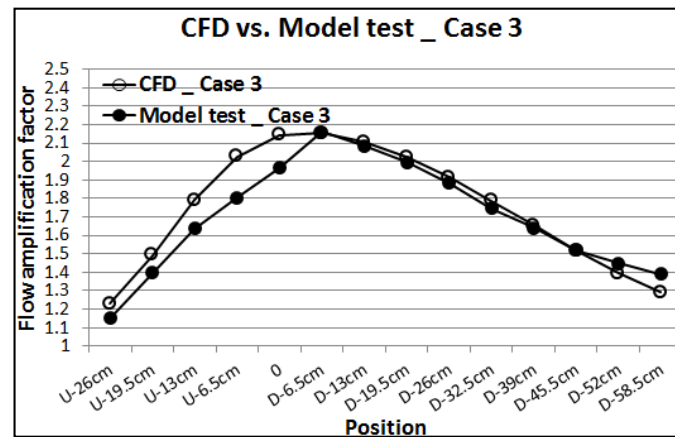


Figure 12. Comparison of CFD and experiment in Case 3.

The maximum error (17%) was found in Case 2. The error seems to be caused by strong vortices near the outlet. However, similar results were found for both CFD and experiment. The locations of the maximum flow speeds occurred were different. In Case 1 and Case 3 ducts, the maximum flow speeds were occurred at “D-6.5 cm”, whereas in Case 2 duct, the maximum flow speed occurred at “0”. That location was affected by the length of the duct. The maximum flow amplification factor was 2.15 in Case 3, the same as the CFD result.

## 6. Conclusions

The duct application has proved the amplification of the flow velocity. The amplification factors for various duct configurations were obtained by CFD. Also, experimental validations were conducted to confirm the CFD analyses. In Case 1, the maximum flow amplification factor was 1.86, while 1.88 was obtained in Case 2 and 2.15 in case 3.

The present research is focused on the duct effect without a turbine to investigate in detail the effects and performance as the base study. Additional research of the duct effect including a turbine installed inside is to be conducted later together with the flow analysis around the various duct configurations. Finally this was a preliminary research study about the duct, so it may be used as a reference and guideline to future duct research. In the future, the installation of a tidal turbine inside the duct will be studied. Wave-current misalignment is also an important factor for application of the duct. This will be the interesting research theme planned for the next stage of our work.

**Acknowledgments:** This work was supported by the New & Renewable Energy Core Technology Program of the Korea Institute of Energy Technology Evaluation and Planning (KETEP), granted financial resource from the Ministry of Trade, Industry & Energy, Republic of Korea (20133030000260). This research was a part of the project titled “Manpower training program for ocean energy”, funded by the Ministry of Oceans and Fisheries, Korea. The authors grateful to INHA University for the funding research grant.

**Author Contributions:** For this work, Do Y. Kim and Su J. Hwang had conducted model experience with the circulation water channel. And Hwang had carried out the CFD analysis and Chan H. Goo analyzed the results from both experience and CFD. Goo and Chul H. Jo had contributed to write this paper. Also, this the written paper was reviewed by Kim and Hwang.

**Conflicts of Interest:** The authors declare no conflict of interest.

## References

1. Bahaj, A.; Batten, W.; McCann, G. Experimental verifications of numerical predictions for the hydrodynamic performance of horizontal axis marine current turbine. *Renew. Energy* **2007**, *32*, 2479–2490. [[CrossRef](#)]
2. Batten, W.M.J.; Hahaj, A.S.; Molland, A.F.; Chaplin, J.R. Hydrodynamics of marine current turbines. *Renew. Energy* **2006**, *32*, 249–256. [[CrossRef](#)]

3. Jo, C.H.; Lee, K.H.; Yim, J.Y.; Chae, K.S. Performance evaluation of TCP device with upstream duct installation. In Proceedings of the Korean Society for Ocean Environment, Yeosu, Korea, 2009; pp. 77–80.
4. Khunthongjan, P.; Janyalertadun, A. A study of diffuser angle effect on ducted water current turbine performance using CFD. *Songklanakarin J. Sci. Technol.* **2012**, *34*, 61–67.
5. Kim, J.W.; Lee, S.H. A study on seawater flow characteristics inside the shrouds used in tidal current generation systems for various geometric angles under constant tidal current velocity. *J. Korean Soc. Coast. Ocean Eng.* **2012**, *24*, 77–83. [[CrossRef](#)]
6. Luquet, R.; Bellevre, D.; Frechou, D.; Perdon, P.; Guinard, P. Design and model testing of an optimized ducted marine current turbine. *Int. J. Mar. Energy* **2013**, *2*, 61–80. [[CrossRef](#)]
7. Lewis, M.; Neill, S.P.; Robins, P.E.; Hashemi, M.R. Resource assessment for future generations of tidal-stream energy arrays. *Energy* **2015**, *83*, 403–415. [[CrossRef](#)]
8. Jo, C.H.; Hwang, S.J.; Lee, K.H.; Goo, C.H. Performance analysis of the duct implemented HAT (horizontal axis turbine) tidal current power system. In Proceedings of the Advanced Maritime Engineering Conference, Hangzhou, China, 28–30 October 2014; p. 450.
9. Jo, C.-H.; Lee, K.-H.; Kim, D.-Y.; Goo, C.-H. Preliminary design and performance analysis of ducted tidal turbine. *J. Adv. Res. Ocean Eng.* **2015**, *1*, 176–185. [[CrossRef](#)]
10. Kim, C.; Lee, N.J.; Hyun, B.S.; Lee, Y.-H. CFD analysis of a counter-rotating tidal current turbine at various rotational speeds within a duct. In Proceedings of the 13th Asian International Conference on Fluid Machinery, Tokyo, Japan, 7–10 September 2015; pp. 13–145.



© 2016 by the authors; licensee MDPI, Basel, Switzerland. This article is an open access article distributed under the terms and conditions of the Creative Commons by Attribution (CC-BY) license (<http://creativecommons.org/licenses/by/4.0/>).